

# Evaluation of the Performance of Vortex Generators on the DU 91-W2-250 Profile using Stereoscopic PIV

**Clara Marika Velte  
Martin Otto Lavér Hansen  
Knud Erik Meyer  
Department of Mechanical Engineering, Technical University of Denmark  
Kgs. Lyngby, 2800, Denmark**

**Peter Fuglsang  
LM Glasfiber  
Lunderskov, 6640, Denmark**

## **ABSTRACT**

Stereoscopic PIV measurements investigating the effect of Vortex Generators on the lift force near stall and on glide ratio at best aerodynamic performance have been carried out in the LM Glasfiber wind tunnel on a DU 91-W2-250 profile. Measurements at two Reynolds numbers were analyzed;  $Re=0.9 \cdot 10^6$  and  $2.4 \cdot 10^6$ . The results show that one can resolve the longitudinal vortex structures generated by the devices and that mixing is created close to the wall, transferring high momentum fluid into the near wall region. It is also seen that the vortex generators successfully can obstruct separation near stall.

**Keywords:** Vortex Generators, Separation Control, Stereoscopic PIV, DU 91-W2-250 Profile and Airfoil.

## **1. INTRODUCTION**

Wind turbine blades must withstand a high out of the rotor plane loading and to absorb the corresponding bending moments a certain thickness is required. It is not uncommon that the innermost airfoils for this reason have a thickness of up to 40% of the chord. Further, there is a limit on how much a blade can be twisted. For these reasons, there will always be separated flow on some part of the blades. To improve the aerodynamic performance of the inner part of the blades carrying most of the loads, aerodynamic devices such as Vortex Generators (VGs) have successfully been used [1]. Vortex generators are series of small winglets that are glued on to the blade shortly upstream of the separated

region. By creating longitudinal vortices, they mix high momentum free stream air into the bottom of the boundary layer, thus delaying separation. Since the flow angles and the airfoil thickness are more well behaved on the outer part, VGs are generally not used here since they, besides from suppressing separation, also yield an increased drag. These devices are sometimes a part of the blade design, but are also used to change unexpected flow separation on already manufactured clean blades. Vortex Generators have many geometrical parameters like general shape, height, length and angle to the main flow direction. Further, it is necessary to specify the chordwise position and spanwise spacing on the blade. In industry, some experience exists for particular blade designs. But if e.g. new airfoils are used, the optimum geometry of the VGs might change. This is associated with some uncertainty and therefore the blade manufacturers are often conservative in their choice of airfoils and in their use of aerodynamic devices. A potential exists to increase the aerodynamic efficiency of wind turbine blades and to decrease the loads and thus lowering the production price for electricity if this uncertainty is lowered by better understanding the physics of how VGs mix high momentum flow into the boundary layer. An ongoing PhD project at the Technical University of Denmark, DTU, aims to analyze the flow structures downstream of VGs in order to gain insight into the physical processes of the flow (see e.g. [2,3]). This may also lead to better numerical methods that can simulate the effect of the VGs and thus constitute a helpful aid in the blade design process.

## 2. METHOD

### Wind tunnel

The wind tunnel, situated at LM Glasfiber in Lunderskov, Denmark, is a closed return system with a contraction ratio of 10:1. The maximum speed is 105 m/s (Mach 0.3), yielding a Reynolds number of  $Re=6.3 \cdot 10^6$  based on a profile of chord 900 mm. The test section (see figure 1) has a width of 1.35 m, a height of 2.70 m and a length of 7 m. A turn table, designed for holding profiles, is located with its center 2915 mm downstream of the test section inlet at its mid-height. The fan is located at the opposite end of the tunnel to the test section and has a maximum power of 1 MW. The tunnel is equipped with a cooling system to keep the temperature on a constant level. A wake rake is mounted on a traverse, which can move in a plane perpendicular to the flow downstream of the turn tables. The test section is equipped with a differential pressure measurement system, which measures 256 pressures: The pressure distribution on the airfoil model, the pressures on floor and ceiling along the test section as well as static and total pressures on the wake rake. Finally, both turn tables have a balance system. The tunnel is designed to have low turbulence intensity in the test section. Measurements at the cross-section of the turntable center reveal a turbulence intensity of about  $Tu=0.09\%$  in the lengthwise component at Reynolds numbers within the range  $Re=3-4.8 \cdot 10^6$  [4].

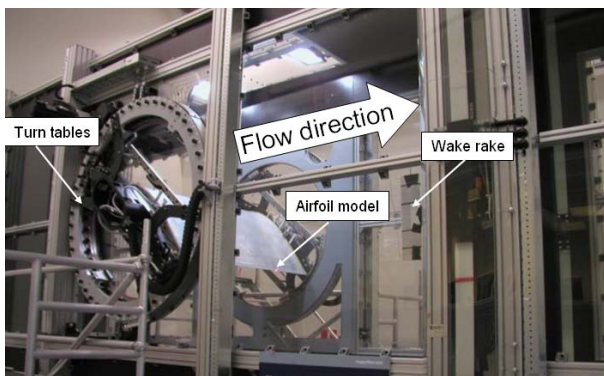


Figure 1. Picture of LM wind tunnel test section.

### DU 91-W2-250 profile

The tests were conducted on the DU 91-W2-250 profile, which is a wind turbine dedicated airfoil developed at Delft University of Technology [5,6]. The chord length of the profile is 900 mm and the span is 1350 mm, which is the same as the width of the test section. Pressure taps were integrated in the profile across the entire chord.

### Actuators

Triangular vanes of height  $h=4.5$  mm and length  $l=2h$  were positioned with an angle of  $\beta=18^\circ$  to the mean flow in a counter-rotating fashion with a distance between the trailing edges of the devices of  $s=3h$  within one pair and  $z=5h$  between each pair, see figure 2. The tests were conducted at two angles of attack;  $\alpha=6.5^\circ$ , corresponding to maximum  $C_L/C_D$  with vortex generators attached at 50% chord and  $\alpha=17.95^\circ$  corresponding to maximum  $C_L$  with vortex generators attached at 20% chord. These angles were found from polar measurements maximizing  $C_L/C_D$  and  $C_L$  for each respective case. The chordwise positioning of the VGs was chosen based on distance to the separation line. Xfoil simulations for  $Re=3.0 \cdot 10^6$  have shown that separation occurs at about 35% chord for an AOA  $\alpha=18^\circ$  with no vortex generators present, whereas separation only occurs at the trailing edge for an AOA  $\alpha=6.5^\circ$ . The optimal vortex generator configurations were found empirically through polar measurements. The boundary layer thickness at  $Re=3.0 \cdot 10^6$  at the position of the vortex generators has been estimated, using CFD, to be about  $\delta=11$  mm at  $x/c=50\%$  for  $\alpha=6^\circ$ . For  $\alpha=18^\circ$  at  $x/c=20\%$  and the same Reynolds number, the boundary layer thickness is estimated to be about  $\delta=6$  mm.

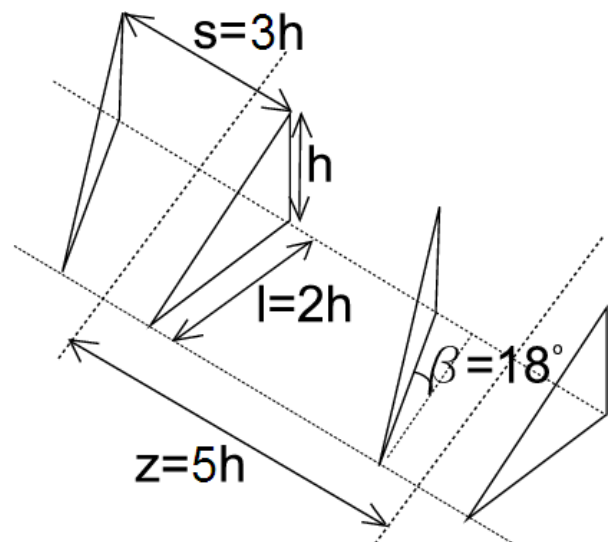


Figure 2. Vortex generator geometry.

### Stereoscopic PIV setup

The stereoscopic PIV equipment included a double cavity NewWave Solo 120XT Nd-YAG laser (wavelength 532 nm), capable of delivering light pulses of 120 mJ. This laser was placed at the side of the test section on the turn table, illuminating the

profile along the span. The light sheet thickness at the measurement position was 1.5 mm. The second pulse of the laser was shifted downstream by approximately 25% in order to increase the dynamic range of the out-of-plane component. The equipment also included two Dantec Dynamics HiSense MkII cameras (1344×1024 pixels) equipped with 60 mm lenses and filters designed to only pass light with wavelengths close to that of the laser light. Both cameras were mounted on Scheimpflug angle adjustable mountings. In order to obtain a smaller measurement area and therefore better spatial resolution, the cameras were equipped with tele-converters. The two cameras were placed on the same side of the light sheet, resulting in one camera placed in the forward scattering direction and one in the backward scattering one. The angle of each respective camera to the laser sheet varied between 32.0°–42.5°. The f-numbers were set to between 4.0 and 5.6 for the camera in the forward scattering direction and was always set to 2.8 for the camera in the backward scattering direction. The seeding consisted of DEHS (Di-Ethyl-Hexyl-Sebacin-Esther) droplets with a diameter of approximately 1–2 μm and was added to the flow downstream of the test section.

#### SPIV data processing

The images were processed using Dantec FlowManager software version 4.7. Adaptive correlation was applied using refinement with an interrogation area size of 32×32 pixels. Local median validation was used in the immediate vicinity of each interrogation area to remove spurious vectors between each refinement step. The overlap between interrogation areas was 50%. The number of recorded velocity fields for the different measurements varied between 1500 and 1800. The recording of image maps was done with an acquisition rate of 2.0 Hz to ensure statistical independency of the samples.

#### Measurement planes

The SPIV measurements were conducted in planes parallel to the span of the wing and normal to the surface at the measurement position of the profile. The measurement positions were primarily determined based on results of numerical simulations, suggesting the location of the separation line. The experiments were conducted at three different free stream velocities,  $U_\infty=15$  m/s, 40 m/s and 60 m/s, corresponding to Reynolds numbers based on profile chord of  $Re=0.9\cdot 10^6$ ,  $2.4\cdot 10^6$  and

$3.6\cdot 10^6$  respectively. The measurement planes with configurations are listed in tables 1 and 2. All measurements are, however, not presented in this paper.  $U_\infty$  is the free stream velocity and  $\Delta X_{VG}/h$  is the distance between the vortex generators and the measurement plane along the surface of the bump normalized by the device height  $h$ . "VGs" indicates that measurements with vortex generators applied have been carried out and "no VGs" indicates measurements without devices.

**Table 1.** Measurement planes for  $\alpha=6.5^\circ$ .

$U_\infty$ (m/s)	$\Delta X_{VG}$	
	20h	40h
15.4	VGs	VGs/no VGs
40.0	VGs	VGs/no VGs
60.0	-	no VGs

**Table 2.** Measurement planes for  $\alpha=17.95^\circ$ .

$U_\infty$ (m/s)	$\Delta X_{VG}$		
	5h	20h	48.2h
15.1	VGs	VGs	VGs/no VGs

### 3. RESULTS AND DISCUSSIONS

#### AOA $\alpha=6.5^\circ$ , maximum $C_L/C_D$

When vortex generators are attached to the blade at 50% chord, polar measurements have shown that  $C_L/C_D$  is maximized for an AOA of  $\alpha=6.5^\circ$ . Figure 3 and 4 show plots of the mean velocity maps for the measurements at  $\Delta X_{VG}/h=40$  with vortex generators for free stream velocities  $U_\infty=15.4$  m/s and  $U_\infty=40.0$  m/s respectively. All three velocity components have been normalized by the free stream velocity  $U_\infty$ . The flow is not fully two-dimensional and therefore velocities along the span of the blade are seen also in the case without devices. It is therefore remarked that the median of the velocity in the spanwise direction has been subtracted from the mean field in order to reveal the structures of the longitudinal vortices generated by the devices. This, however, results in large spanwise velocity vectors close to the wall. One can also see some reflections from the vortex generators as spurious vectors occurring periodically throughout the span. One can clearly see the structures of the longitudinal vortices generated and accordingly a redistribution of the axial velocity close to the wall. It is therefore possible to resolve these structures using SPIV. The flow field shows quite similar behavior at  $U_\infty=15.4$  m/s and  $U_\infty=40.0$  m/s.

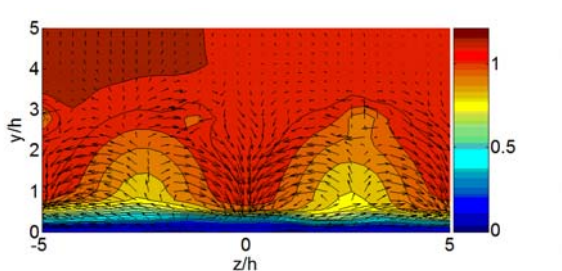


**Figure 3.** Mean velocity vector map for AOA  $\alpha=6.5^\circ$  and free stream velocity  $U_\infty=15.4$  m/s at  $\Delta X_{VG}/h=40$ .

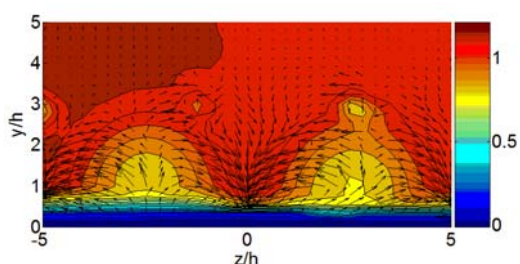


**Figure 4.** Mean velocity vector map for AOA  $\alpha=6.5^\circ$  and free stream velocity  $U_\infty=40.0$  m/s at  $\Delta X_{VG}/h=40$ .

Figures 5 and 6 show the spanwise averaged velocity profiles from the mean velocity field for the case with and without devices as well as profiles from the mean velocity field extracted in the upwash and downwash regions generated by the vortex generators. It seems that the negative effect in the upwash region is higher than the positive effect in the downwash region. This is also reflected in the spanwise averaged velocity.

#### AOA $\alpha=17.95^\circ$ , maximum $C_L$

When vortex generators are attached to the blade at 20% chord, polar measurements have shown that  $C_L$  is maximized for an AOA of  $\alpha=17.95^\circ$ . Figure 7 shows spanwise averaged axial velocity profiles at  $\Delta X_{VG}/h=48.2$  (corresponding to 45% chord) for free stream velocities  $U_\infty=15.1$  m/s with and without vortex generators applied respectively. The velocity has been normalized by the free stream velocity  $U_\infty$ . The effect of the vortex generators on the flow can be seen in the respect that the averaged velocities at all measurement points are positive when the vortex generators are applied as opposed to the neutral case where separation occurs. At this station it is no longer possible to see the structures of the vortices, but the separation hampering effect is still significant.

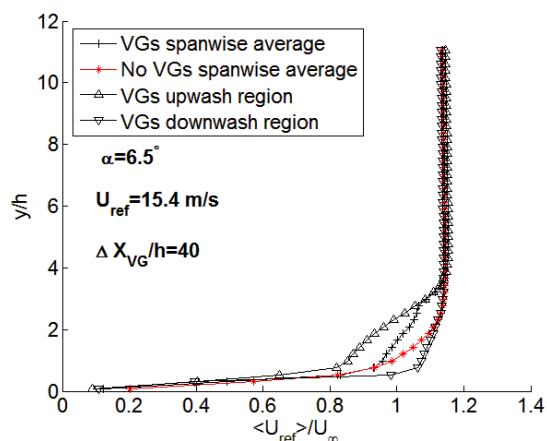


**Figure 5.** Velocity profiles for  $\alpha=6.5^\circ$ ,  $U_\infty=15.4$  m/s and  $\Delta X_{VG}/h=40$ . The figure displays spanwise averaged velocity profiles from the mean velocity field with and without devices attached as well as profiles from the mean velocity field extracted in the upwash and downwash regions.

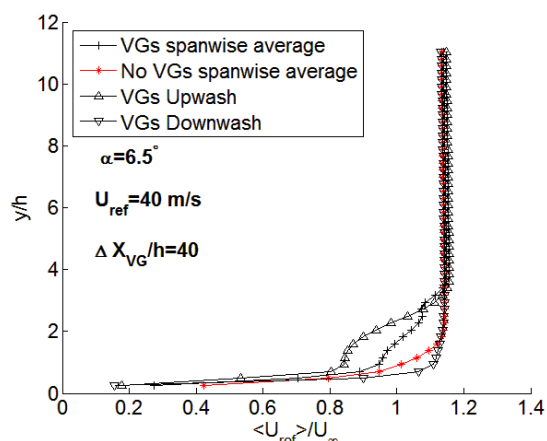


**Figure 6.** Velocity profiles for  $\alpha=6.5^\circ$ ,  $U_\infty=40.0$  m/s and  $\Delta X_{VG}/h=40$ . The figure displays spanwise averaged velocity profiles from the mean velocity field with and without devices attached as well as profiles from the mean velocity field extracted in the upwash and downwash regions.

## 4. CONCLUSIONS

The results have shown that one can measure and resolve the large scale flow structures created by Vortex Generators on a DU 91-W2-250 profile at a Reynolds numbers of  $Re=0.9 \cdot 10^6$  and  $2.4 \cdot 10^6$  and AOA of  $\alpha=6.5^\circ$ . The effect is qualitatively the same for the two Reynolds numbers. For an AOA of

$\alpha=17.95^\circ$  at 48.2 device heights downstream of the VGs (45% chord), the effect of the Vortex Generators is significant and the results show an elimination of separation in a time- and spanwise average. At this station the vortex structures can no longer be clearly distinguished.

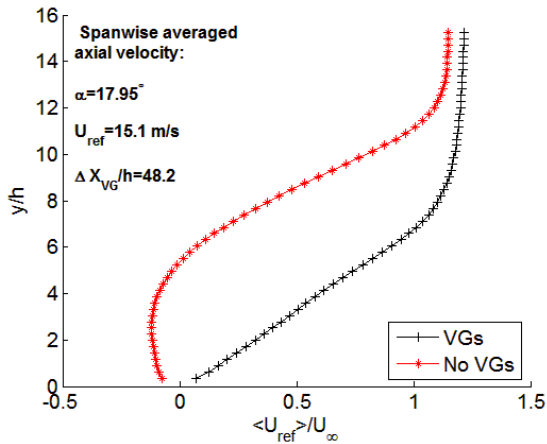


**Figure 7.** Spanwise averaged axial velocity for AOA  $\alpha=17.95^\circ$  and free stream velocity  $U_\infty=15.1$  m/s at  $\Delta X_{VG}/h=48.2$ .

## 5. REFERENCES

- [1] S. Øye, The Effect of Vortex Generators on the Performance of the ELKRAFT 1000 kW Turbine, **9th IEA Symposium on Aerodynamics of Wind Turbines Stockholm, Sweden, ISSN 0590-8809, 1995.**
- [2] C. M. Velte, M. O. L. Hansen and D. Cavar, Flow analysis of vortex generators on wing sections by stereoscopic particle image velocimetry measurements, **Environ. Res. Lett.**, 3, 015006, 2008.
- [3] C. M. Velte, M. O. L. Hansen and K. Jønck, Experimental and numerical investigation of the performance of vortex generators on separation control, **J. Phys.: Conf. Ser.** 75 (11pp), 2007.
- [4] H-D. Papenfuß, Aerodynamic Commissioning of the New Wind Tunnel at LM Glasfiber A/S (Lunderskov), **LM Glasfiber Technical report Lunderskov, Denmark, 2006.**
- [5] W. A. Timmer and R. P. J. O. M. van Rooij, Summary of the Delft University Wind Turbine Dedicated Airfoils, **AIAA-2003-0352**, 2003.
- [6] R. P. J. O. M. van Rooij and W. A. Timmer, Roughness Sensitivity Considerations for Thick Rotor Blade Airfoils, **AIAA-2003-0350**, 2003.